This full text paper was peer-reviewed at the direction of IEEE Instrumentation and Measurement Society prior to the acceptance and publication.

Novel Telemetric Technique for Passive Resistive Sensors Based on Impedance Phase Angle Measurement at Constant Frequency

Michele Bona*, Michela Borghetti, Emilio Sardini, Mauro Serpelloni
Department of Information Engineering, University of Brescia, Via Branze 38, 25123 - Brescia, Italy
*Corresponding author: +39 0303715937, e-mail address: m.bona002@unibs.it

***Abstract*— Telemetric systems are a valid alternative to measurement devices exploiting batteries or cabled connections, which may be not suitable in some cases, such as in harsh or hermetic measurement environments. They permit either to supply a passive sensor or to carry out monitoring tasks without contact. In this paper, we propose a novel measurement technique for telemetric systems working with a resistive sensing element. Such technique is based on a reading of system impedance phase angle always at sensing inductor's resonant frequency, while relative distance between system inductors is kept fixed. Analytical expressions have been derived to calculate sensor resistive output from phase angle value. They have been obtained from a proper circuit model of the telemetric device. The proposed method has been applied to the wireless measurement of temperature inside an oven. Experimental tests have been carried out, by putting a resistive sensor inside the oven and increasing its internal temperature from about 28 °C to about 134 °C. Preliminary results show that calculated temperature values present an average deviation from reference equal to 1.7 °C. Furthermore, uncertainty related to such values is 1.2 °C. Therefore, they prove the feasibility of implementing the proposed technique in all the applications that require the use of telemetric devices with passive resistive sensors.**

Keywords*— *Temperature measurement; Telemetric device; Resistive sensor; Impedance phase angle; Constant frequency.

I. INTRODUCTION

In some cases, such as in harsh or hermetic environments, electronic measurement systems based on batteries or wired connections are not suitable. In these cases, interesting and attractive opportunities come from telemetric devices. In such systems, a readout unit is connected to an inductor, which couples magnetically to another inductor that forms a completely passive sensing circuit with a sensor. Such inductive coupling permits wireless sensor supply by readout unit and data transmission to it. In this way, passive sensing circuit is placed inside measurement environment. On the other hand, readout unit is located outside, i.e. in a safer position, since it contains all the electronics to elaborate sensor output. Therefore, there is no need for elements such as cabled connections, batteries or active circuits, which could cause local perturbations in the environment or risk to fail inside it.

Telemetric devices are employed for the wireless measurement of multiple physical and chemical quantities. Examples touch pressure [1]-[2], temperature [3]-[4], humidity [5]-[6], strain [7]-[8], pH [9], and the presence of gases [10]. Furthermore, they are realized through different manufacturing technologies, according to the operation requirements of the specific application for which they are designed. For instance, passive sensing circuit can be fabricated with materials that keep their physical and chemical properties stable even in harsh conditions, like Low Temperature Co-fired Ceramics (LTCC) [1], [10]. In other cases, passive elements are printed directly on a flexible substrate [2]-[3]. In this way, they fit surfaces with different shapes. Finally, sensor can be designed as a microelectromechanical system (MEMS) [1], [3]-[4] with reduced dimensions, in order to occupy small spaces.

Literature reports telemetric systems equipped with capacitive [1], [4]-[7], [9]-[10], inductive [2], [8], or resistive [3] sensors. Thus, passive sensing circuits have a LC (in the first and second cases) or LR (in the third one) configuration. The former is the most considered solution, whereas the latter is less investigated. Anyway, the corresponding measurement techniques are based on system frequency analyses to detect circuit resonances, which shift according to sensor output change. However, such methods imply performing continuous frequency sweeps, in order to identify the resonances. This results in an increase of measurement time and complexity of the electronics that composes the readout unit.

On the contrary, this paper proposes an alternative technique for telemetric devices operating with a high-value resistive sensor, i.e., whose output is in the order of the kiloohm. The proposed method relies on a mathematical formula that expresses the relationship between sensor output, the other device elements, and a reading of system electrical impedance, executed always at the same frequency. The first part of the work will present the analysis carried out to derive our solution from a proper circuit model of the system. Then, the technique has been applied for wireless temperature measurement inside a hermetic environment. Therefore, the second part will describe the experimental tests carried out on a real apparatus and the achieved results.

978-1-5090-3596-0/17/$31.00 ©2017 IEEE

II. Measurement technique

A. Telemetric system model

A new circuit model is proposed to describe a telemetric system with a high-value resistive sensor. It is a lumped-parameter model that includes the parasitic effects and magnetic flux exchange between readout inductor and sensing inductor, which are connected to readout unit and passive sensor, respectively. This model is illustrated in Fig. 1, where each element is identified with the corresponding physical principle. Elements have the following definition [11]. Inductances L_R and L_S symbolize leakage fluxes from readout and sensing inductors, respectively. On the contrary, L_M represents the flux exchanged between them. These parameters depend on the distance at which inductors are coupled [12]. Parasitic resistance R_2 takes into account the losses in sensing inductor's windings, because of Joule effect. On the other side, parasitic capacitance C_2 represents the electric field generated between the windings of sensing inductor and between windings and its substrate [11]. Then, C_x is a fixed capacitor that can be attached in parallel to sensing inductor, in order to set its resonant frequency. Resistance R_x models sensor output, which varies as a function of the measured quantity. It can assume values from about a kiloohm up to some tens of kiloohm. Finally, coefficient n is the windings ratio.

Combining the elements of the model of Fig. 1 permits to obtain the expression of impedance at readout inductor's terminals (which is indicated with "Z" in Fig. 1). It is reported in (1) as a function of frequency f. Parameter C_p is the sum between C_2 and C_x. L_1 and L_2 are the equivalent inductances for readout and sensing inductors, respectively. They are linked to model elements through the following relations [11]:

$$L_1 = L_M + L_R \tag{2}$$

$$L_2 = L_S + L_M / n^2 \tag{3}$$

L_1 and L_2 are constant parameters. In particular, they are not affected by the relative position between the inductors, since leakage flux growth when inductors get far is perfectly compensated by coupling flux decrease, and vice versa.

Finally, variable β depends on L_M, as defined by (4). Thus, it changes if relative position between the inductors varies.

$$\beta = \frac{L_M^2}{L_2 n^2} \tag{4}$$

Used notation with L_R, L_S, L_M, and β is equivalent at all, from a mathematical point of view, to the more common representation employing coupling factor to model the interaction between the inductors [1], [3], [7], [9]-[10].

B. Study on impedance phase angle

Equation (1) provides some information on how Z varies with system parameters and, therefore, with R_x. Conversely, we started from such expression to find an equation that

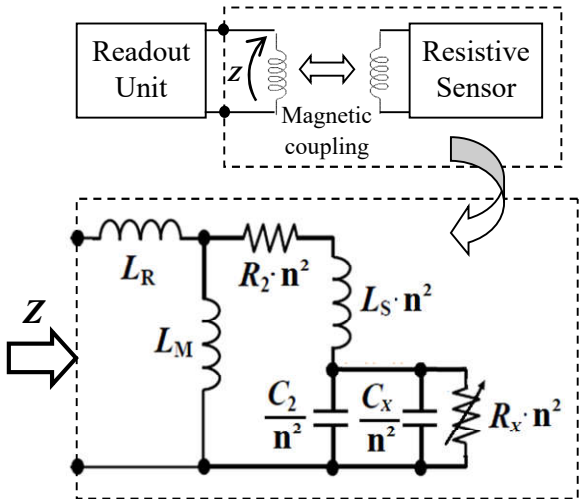

Fig. 1. System circuit model used to derive the mathematical equations of the proposed measurement technique.

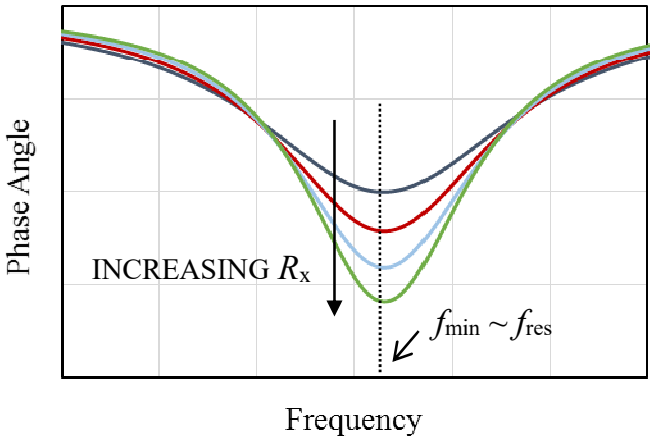

Fig. 2. Qualitative curves representing how impedance phase angle of a telemetric system varies when the output of its resistive sensor increases. They reproduce the results achieved in [13].

allowed us calculating sensor output from an impedance measurement performed at readout inductor's terminals. For this purpose, we evaluated which impedance point was the most suitable to detect. In a previous work [13], we studied the response of a telemetric device when the value of its resistive sensing element changed. In particular, we represented its impedance as magnitude and phase angle. Fig. 2 reproduces the results related to the latter. Reported qualitative curves show how it behaves when R_x augments. We found that phase angle decreased when sensor output increased. In particular, its minimum was a convenient point, since its variation with R_x presented a linear trend, for sensor output range in the order of some kiloohms. In addition, the corresponding frequency f_{min} presented a change with respect to its starting value equal to 0.12% at most. References [10, 13] report similar findings.

Equation (1)

$$Z(j2\pi f) = \frac{-4\pi^2(L_1L_2 - L_2\beta + R_xC_pL_1R_2)f^2 + j2\pi L_1(R_2 + R_x)f - j8\pi^3 R_xC_pL_2(L_1 - \beta)f^3}{(R_2 + R_x) - 4\pi^2 R_xC_pL_2f^2 + j2\pi(L_2 + R_xC_pR_2)f} \tag{1}$$

Therefore, f_{min} can be considered constant. If coupling distance between the inductors is sufficient, then f_{min} can be identified with sensing inductor's resonant frequency f_{res} [1], with further addition of capacitance C_x. This frequency is defined as:

$$f_{res} = \frac{1}{2\pi\sqrt{L_2 C_p}} \tag{5}$$

Therefore, we based our measurement technique on a phase angle reading performed always at f_{res}. Working at a fixed frequency leads to some advantages related to the aspect that a complete sweep for the identification of the frequencies of interest is not necessary. Thus, both measurement time and readout electronics complexity can be reduced.

C. Mathematical analysis

Equation (6) provides phase angle mathematical function of frequency f. It is derived from (1).

$$\angle Z(f) = \frac{\pi}{2} - a\tan 2\left[\frac{2\pi(L_2 + R_x C_p R_2)f}{R_2 + R_x - 4\pi^2 R_x C_p L_2 f^2}\right] + \\ + a\tan 2\left[\frac{2\pi(L_1 L_2 - L_2\beta + R_x C_p L_1 R_2)f}{L_1(R_2 + R_x) - 4\pi^2 R_x C_p L_2 (L_1 - \beta) f^2}\right], \tag{6}$$

Since the proposed method is supposed to be applied for telemetric systems operating with resistive sensors in the order of the kiloohm, then R_x is much greater than R_2. In fact, such parasitic resistance is usually in the order of some ohms or tens of ohm. Therefore, this approximation can be introduced:

$$R_x + R_2 \cong R_x \tag{7}$$

Then, phase angle at frequency f_{res} is called φ from now on:

$$\varphi = \angle Z(f = f_{res}) \tag{8}$$

Equation (6) is used to calculate the expression of the tangent of φ, taking into account also (7) and (8):

$$\tan(\varphi) = \frac{L_2(L_1 - \beta) + L_1 R_2 C_p R_x}{\beta R_x \sqrt{L_2 C_p}} \tag{9}$$

Working at f_{res}, together with considering (7), permits to simplify (6) in a significant way, when obtaining (9). Finally, (9) is reordered to isolate sensor output:

$$R_x = \frac{L_2(L_1 - \beta)}{\beta\sqrt{L_2 C_p}\tan(\varphi) - L_1 C_p R_2} \tag{10}$$

Analytical formula provided by (10) permits to calculate sensor output starting from a reading of impedance phase angle carried out always at fixed frequency f_{res}. In fact, it expresses the relationship between R_x, φ, and the other system parameters. L_2, R_2, and C_2 are the elements of the equivalent electrical circuit representing sensing inductor with a series between an inductance and a resistance, in parallel with a capacitance [11]. These parameters depend on inductors' geometry [14], and they can be obtained through a specific measurement. The same thing is valid for L_1. Then, capacitance C_x is a component chosen by system designer to adjust f_{res}, as previously mentioned. Finally, parameter β increases if inductors get closer when they are coupled, as it depends on L_M. Yet, if inductors' relative position remains fixed during the entire measurement process, then β is constant. However, L_M direct estimation is not immediate to obtain. Anyway, we considered an alternative approach, which implies to find β in an indirect manner, i.e., by reading φ at a known condition and implementing the following formula:

$$\beta = \frac{L_1(L_2 + R_{x,0} C_p R_2)}{R_{x,0}\sqrt{L_2 C_p}\tan(\varphi_0) + L_2} \tag{11}$$

where $R_{x,0}$ is sensor output in correspondence of this known condition, whereas φ_0 is the related phase angle detected at f_{res}. We obtained (11) by reordering the terms of (9) to isolate β.

In conclusion, the proposed measurement method consists in the following steps. First, inductors are taken separately and the elements of their equivalent circuits are measured. If necessary, a capacitor is added in parallel to sensing inductor in order to act as variable C_x. Parameters L_2 and C_p define working frequency f_{res} through the implementation of (5). Second, inductors are coupled at a fixed relative position. Parameter β is calculated through a single-point system calibration, by applying (11) starting from a known condition. Finally, real measurement procedure begins. While system is in operation, φ is detected, and R_x is calculated from (10).

III. Application to Temperature Measurement

A. Experimental setup

We carried out an experimental analysis to apply the proposed technique to the wireless measurement of temperature in a hermetic environment. Fig. 3 reports a block scheme of the experimental setup realized for the analysis, whereas Fig. 4 shows an image with some of its components.

We employed a telemetric configuration made by two planar inductors. They were fabricated through printed circuit board (PCB) technology, by patterning a square copper spiral on a rigid substrate of FR4 glass-reinforced epoxy. Table I lists their geometric and electrical characteristics. The latter are the elements of inductors' equivalent circuits. They were measured with an HP4194A impedance analyzer. We derived the uncertainty associated to the electrical characteristics by taking into account analyzer's accuracy in their estimation. It refers to a 95% confidence interval (CI). In Table I, the electrical characteristics related to sensing inductor comprise the addition of a 560 pF commercial capacitor, which works as C_x. According to the measured values of Table I and Eq. (5), frequency f_{res} was equal to about 2.52 MHz.

A Class A (according to standard EN 60751) Pt1000 resistive temperature sensor was connected to sensing inductor and capacitor C_x. These components form system's sensing circuit, which was put in an oven, as shown in the inset of Fig. 4. The oven simulates a hermetic environment, where temperature is supposed to be measured.

We placed readout inductor near the closed oven, keeping it parallel and coaxial with respect to sensing inductor, at a

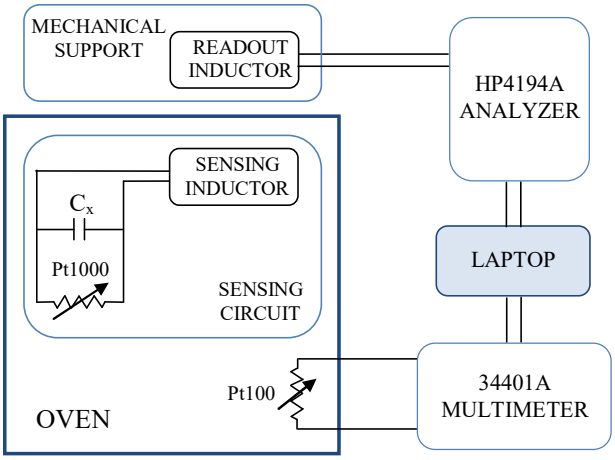

Fig. 3. Block scheme of the used experimental apparatus.

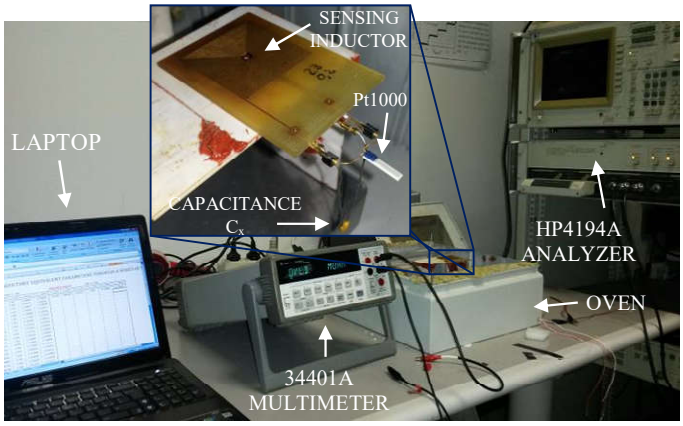

Fig. 4. Picture showing the experimental apparatus.

relative distance fixed to 20 mm, thanks to a mechanical support equipped with micrometric screws. Readout inductor's terminals were then connected to HP4194A analyzer, which was interfaced to a laptop via a GPIB-USB high-speed module. A Virtual Instrument (VI) written in LabVIEW was executed on laptop for data acquisition from HP4194A analyzer and their elaboration. The ensemble made by these two instruments compose system's readout unit. In addition, another resistive temperature sensor, a Class A Pt100, was inserted in the oven. It was exploited as a reference, to make a comparison with the results provided by the proposed method. It was connected to an Agilent 34401A digital multimeter, which was interfaced to the laptop and was driven by the same VI. Thus, a synchronized data acquisition from the two devices was achieved.

B. Measurement protocol

Process first step consisted in system single-point calibration. Room temperature (i.e., the initial state) was chosen as known condition. After a trigger command from laptop, HP4194A analyzer detected φ_0. Then, the VI received the data from that reading and calculated β, by applying (11),

TABLE I. INDUCTORS' CHARACTERISTICS

Property	Value (unit) Readout's	Value (unit) Sensing's (*)
Geometric characteristics		
outer side	50 (mm)	27 (mm)
inner side	27 (mm)	4 (mm)
number of windings	28	23
windings width	150 (µm)	300 (µm)
windings spacing	250 (µm)	200 (µm)
Electrical characteristics		
equivalent inductance	47.48 ± 0.09 (µH)	7.05 ± 0.01 (µH)
equivalent resistance	35.10 ± 0.02 (Ω)	1.899 ± 0.004 (Ω)
equivalent capacitance	3.062 ± 0.006 (pF)	566.6 ± 1.1 (pF)

(*) Parallel capacitance is included for electrical parameters estimation

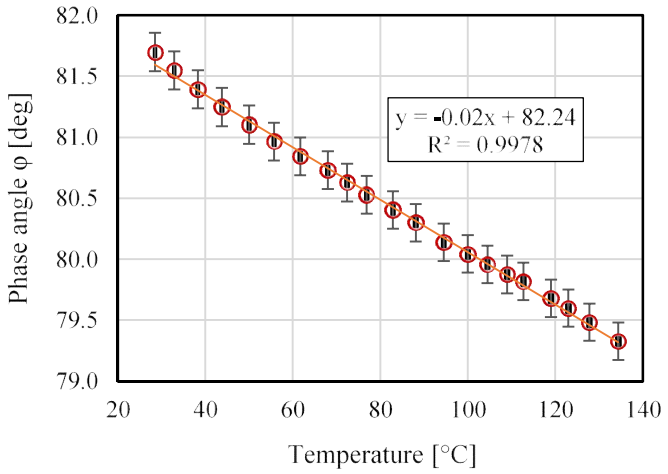

Fig. 5. Phase angle φ as a function of temperature.

from system parameters and sensor output $R_{x,0}$, which was found from its datasheet.

Afterwards, the VI began to operate in continuous mode, and the real measurement procedure started. HP4194 analyzer identified φ. Subsequently, the VI calculated R_x by implementing (10), from system parameters and coefficient β obtained earlier. Then, it converted R_x into a temperature value, by exploiting sensor linear relationship, which is known from its datasheet. Finally, it compared calculated temperature with reference provided by Pt100 and digital multimeter. While system was working, we gave growing heat to the oven, increasing gradually its temperature from about 28 °C to about 134 °C corresponding to a variation from about 1111 Ω to about 1515 Ω.

C. Preliminary results

The experimental tests carried out so far permitted us to obtain preliminary results about method effectiveness in estimating resistive sensor output.

Fig. 5 reports some of the read values of phase angle φ as a function of temperature. The vertical bars show the uncertainty related to φ measurement, which is affected by

two factors. These are analyzer's accuracy and f_{res} value calculation (which depends on the uncertainty on L_2 and C_p). On the other hand, the horizontal bars (which are barely visible in Fig. 5) derive from the uncertainty on reference temperature. Such uncertainty is affected by Pt100's tolerance characteristics and digital multimeter's measurement accuracy. In both cases, uncertainty refers to a 95% CI. Fig. 5 points out how φ decreases when temperature grows, since resistive sensor output increases as well. This confirms the trend shown in Fig. 2. Phase angle behavior is almost linear within the temperature range that we took into account. Indeed, a linear regression fits the points with a coefficient of determination R^2 close to 0.998. We found that φ changed from 81.70 ± 0.16 degrees to 79.33 ± 0.15 degrees for a temperature increase from 28.5 ± 0.2 °C to 134.4 ± 0.5 °C. This means that φ sensitivity to temperature is equal to 0.022 degrees/°C, on average.

Fig. 6 shows the values of temperature calculated by implementing the proposed method from phase angle points reported in Fig. 5. In addition, bars referring to temperature uncertainty for a 95% CI are included. Furthermore, Fig. 6 compares calculated values with reference. Fig. 6 points out how the two series are close to each other. Indeed, their difference is equal to 1.7 °C on average. In general, it is between 0.2 °C and 3.7 °C along all the studied temperature range. Furthermore, uncertainty on calculated temperature results to be equal to 1.2 °C, on average. It was estimated by applying the rules of the "Guide to the expression of Uncertainty in Measurement" (GUM) to the mathematical equations illustrated in Section II, starting from the uncertainty related to φ measurement and system parameters. We took into account Pt1000's tolerance characteristics at the same time. Therefore, final uncertainty is affected by all these factors, which were previously described. Achieved results are satisfying, considering also the examined range, which is quite wide. They prove that calculating the output of a resistive sensor through the proposed solution is a valid approach.

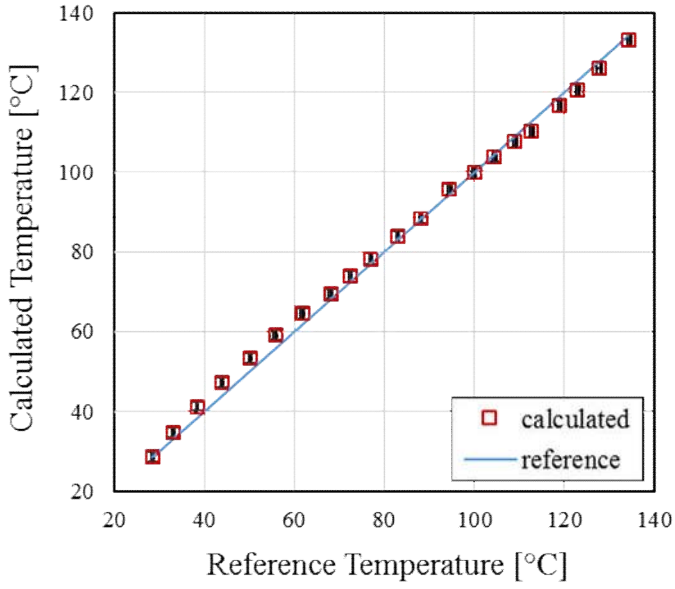

Fig. 6. Comparison between calculated and reference values of temperature.

IV. Conclusions

This paper has presented a novel measurement technique for telemetric systems that work with passive high-value resistive sensors. It is based on two features. The first one is a reading of impedance phase angle always at the frequency identifying sensing inductor's resonance, keeping system inductors at a fixed relative position. The second one is the implementation of equations that permit to calculate sensor output remotely from such reading and system parameters. We described how we derived these mathematical formulas from a proper circuit model of the system. Furthermore, the proposed solution has been applied to the wireless measurement of temperature inside an oven. For this purpose, we used a real telemetric device made of PCB planar inductors and a Pt1000 resistive sensor. Performed experimental analysis has shown that method provides a temperature estimation that deviates of 1.7 °C from reference, on average. Furthermore, derived uncertainty on calculated temperature is 1.2 °C. Such results point out the feasibility of working at a constant frequency. This has the advantage of avoiding continuous sweeps to identify the frequencies of interest. In general, results demonstrate the validity of our approach, which could represent a useful alternative, especially when a direct estimation of the output of a resistive sensor is not possible to obtain because of the characteristics of measurement environment.

Future studies will investigate the possibility to find a way to compensate the influence of a change in inductors' relative position (as achieved in [11] for devices that operate with capacitive sensing elements). In fact, this could overcome the limitation due to the necessity of always maintaining the inductors at a fixed relative position during the entire measurement process.

Acknowledgment

The activity has been financed by Cluster project "Smart Adaptive Manufacturing" CTN_01_00163_216730.

References

[1] M. A. Fonseca, J. M. English, M. von Arx, and M. G. Allen "Wireless micromachined ceramic pressure sensor for high-temperature applications," J. Microelectromech. Syst., vol. 11, no. 4, pp. 337–343, 2002.

[2] G.-Z. Chen, I.-S. Chan, L. K. K. Leung, and D. C. C. Lam, "Soft wereable contact lens sensor for continuous intraocular pressure monitoring," Med. Eng. Phys., vol. 36, pp. 1134–1139, 2014.

[3] M. Lee, K. Morimoto, and Y. Suzuki, "Flexible wireless wall temperature sensor for unsteady thermal field," J. Phys. Conf. Ser. vol. 660, p. 012019, 2015.

[4] B. Andò, S. Baglio, N. Savalli, and C. Trigona, "Cascaded "triple-bent-beam" MEMS sensor for contactless temperature measurements in nonaccessible environments," IEEE Trans. Instrum. Meas., vol. 60, no. 4, pp. 1348–1357, 2011.

[5] E. L. Tan, W. N. Ng, R. Shao, B. D. Pareles, and K. G. Ong, "A wireless, passive sensor for quantifying packaged food quality," Sensors, vol. 7, pp. 1747–1756, 2007.

[6] D. Marioli, E. Sardini, and M. Serpelloni, "An inductive telemetric measurement system for humidity sensing," Meas. Sci. Technol., vol. 19, p. 115204, 2008.

[7] Y. Jia, F. J. Agosto, and M. T. Quiñones, “Design and characterization of a passive wireless strain sensor,” Meas. Sci. Technol., vol. 17, pp. 2869–2876, 2006.

[8] J. C. Butler, A. J. Vigliotti, F. W. Verdi, and S. M. Walsh, “Wireless, passive, resonant-circuit, inductively coupled, inductive strain sensor,” Sens. Actuators A, Phys., vol. 102, pp. 61–66, 2002.

[9] S. Bhadra, W. Blunt, C. Dynowski, M. McDonald, D. J. Thomson, M. S. Freund, N. Cicek, and G. E. Bridges, “Fluid embeddable coupled coil sensor for wireless pH monitoring in a bioreactor,” IEEE Trans. Instrum. Meas., vol. 63, no. 5, pp. 1337–1346, 2014.

[10] M. Ma, Z. Liu, W. Shan, Y. Li, K. Kalantar-zadeh, and W. Wlodarski, “Passive wireless gas sensors based on the LTCC technique,” in Proc. 2015 IEEE MTT-S IMWS-AMP, 2015, pp. 1–3.

[11] D. Marioli, E. Sardini, M. Serpelloni, and A. Taroni, “A new measurement method for capacitance transducers in a distance compensated telemetric sensor system,” Meas. Sci. Technol., vol. 16, pp. 1593–1599, 2005.

[12] D. Marioli, E. Sardini, M. Serpelloni, and A. Taroni, “Contactless trasmission of measurement information between sensor and conditioning electronics,” IEEE Trans. Instrum. Meas., vol. 57, no. 2, pp. 303–308, 2008.

[13] M. Bona, E. Sardini, M. Serpelloni, B. Andò, and C. O. Lombardo, “Study on a telemetric system that works with an inkjet-printed strain gauge,” in Proc. IEEE SAS, 2016, pp. 338–343.

[14] U.-M. Jow, and M. Ghovanloo, “Design and optimization of printed spiral coils for efficient transcutaneous inductive power transmission,” IEEE Trans. Biomed. Circuits Syst., vol. 1, no. 3, 193–202, 2007.